

# Reversible Immuno-Infrared Sensor for the Detection of Alzheimer's Disease Related Biomarkers

Brian Budde,<sup>†,‡,⊥</sup> Jonas Schartner,<sup>†,‡,⊥</sup> Lars Tönges,<sup>§,⊥</sup> Carsten Kötting,<sup>\*,†,‡,⊥</sup> Andreas Nabers,<sup>†,‡</sup> and Klaus Gerwert<sup>†,‡</sup>

<sup>†</sup>Department of Biophysics, Ruhr-Universität Bochum, Universitätsstrasse 150, D-44801 Bochum, Germany

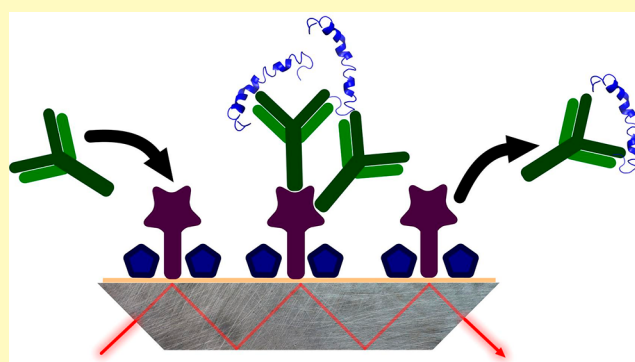
<sup>§</sup>Department of Neurology, Ruhr-Universität Bochum, St. Josef-Hospital, Gudrunstrasse 56, D-44791 Bochum, Germany

<sup>⊥</sup>Center for Protein Diagnostics (ProDi), Gesundheitscampus 4, 44801 Bochum, Germany

## S Supporting Information

**ABSTRACT:** The development of biosensors for medical purposes is a growing field. An immuno-infrared biosensor for the preclinical detection of Alzheimer's disease (AD) in body fluids was developed. The key element of this sensor is an ATR crystal with chemically modified surface to catch the biomarker out of the body fluid. So far, the immuno-infrared sensor can be used only once and requires time-consuming steps of sensor exchange, sensor cleaning, and novel surface functionalization. Here, we developed an immuno-infrared sensor providing a reusable surface and showcase its performance by the detection of the AD biomarker proteins A $\beta$  and Tau in human cerebrospinal fluid (CSF). The sensor surface is covalently coated with the immunoglobulin binding proteins Protein A or Protein G. These were employed for noncovalent immobilization of antibodies and the subsequent immobilization and analysis of their antigens. The reversible antibody immobilization can be repeated several times with the same or different antibodies. Further, the more specific binding of the antibody via its Fc region instead of the conventional NHS coupling leads to a 3–4-fold higher antigen binding capacity of the antibody. Thus, the throughput, sensitivity, and automation capacity of the immuno-infrared biosensor are significantly increased as compared to former immuno-infrared assays. This immuno-sensor can be used with any antibody that binds to Protein A or Protein G.

**KEYWORDS:** regenerative biosensors, immuno-infrared sensor, ATR-FTIR spectroscopy, biomarker detection, amyloid-beta and tau, body fluids, neurodegenerative diseases, Alzheimer's disease



Alzheimer's disease (AD) is the most common neurodegenerative disease. Early diagnosis of AD is a key factor for future therapies. Today, disease related biomarkers such as Amyloid- $\beta$  (A $\beta$ ) and Tau are measured in cerebrospinal fluid (CSF) and recently in blood.<sup>1–4</sup> Already in 2016, an immuno-infrared sensor was applied to detect the A $\beta$  secondary structure distribution in CSF and blood plasma of moderate to severe AD cases and disease control subjects.<sup>1,2</sup> In 2018, the sensor was validated also for the identification of preclinical AD stages in an average of 8 years before clinical manifestation with a sensitivity of 71% and specificity of 91%.<sup>3</sup> Most recently, combination of plasma and CSF A $\beta$  and Tau analyses yielded a sensitivity of 87% and specificity of 97%.<sup>4</sup> This sensor is based on an antibody functionalized surface where antibodies are covalently attached. An easy regeneration of the biosensor surface will significantly enhance its applicability. Surfaces often have to be immersed into harsh chemicals, are polished, or even discarded. Thus, reusing the sensor surface is limited.

In most immunoassays, such as ELISA, antibodies are unspecifically adsorbed or covalently bound to surfaces with

random orientation<sup>1,5,6</sup> which can influence the efficiency of antigen binding.<sup>7</sup> Immunoglobulin binding proteins show promising properties toward specific and reversible binding of antibodies.<sup>8–11</sup> A noncovalent immobilization of specific IgG antibodies via Protein A and G leads to a distinct orientated antibody layer on the surface. Protein A and G mediate a high affinity interaction with the Fc constant region of the IgG antibody, which is reversible using chemical treatment, e.g., pH change.<sup>12</sup>

Here, we introduce Protein A and G as capturing agent on ATR-Germanium crystals. This new assay provides a reversible platform for rapid and robust analyses of human blood and CSF samples for AD diagnosis.

**Received:** April 3, 2019

**Accepted:** June 26, 2019

**Published:** June 26, 2019

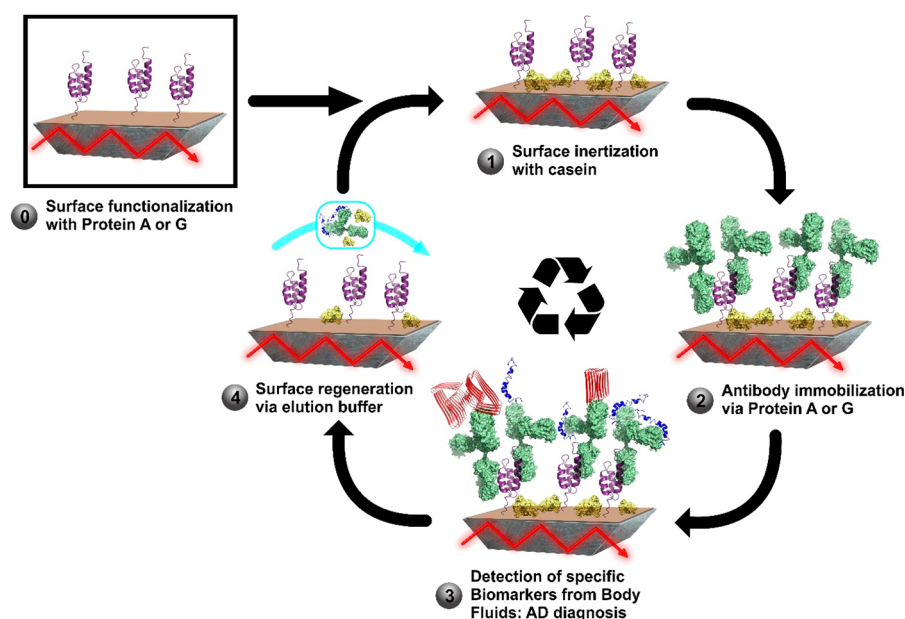


**Figure 1.** General principle of the reversible immuno-infrared assay. First, immunoglobulin binding proteins such as Protein A or G are covalently coupled to the sensor surface via silane chemistry (step zero). Free reactive sites on the surface are saturated with blocking solution (step one) before antibody immobilization (step two). The functionalized sensor can be used, for example, for the detection of AD biomarkers in aqueous solution or body fluids for AD diagnosis (step three). Finally, antigen–antibody complexes can be removed with elution buffer (step 4) and the sensor can be reused by starting with step 1.

## EXPERIMENTAL SECTION

**Surface Modification of Germanium.** The surface modification of ATR-germanium crystals via silane chemistry was described previously.<sup>1,3,13</sup> Briefly, the germanium crystals were incubated for 10 min in 90%  $\text{H}_2\text{O}_2$ /10% oxalic acid. Afterward, ATR-crystals were incubated with 300  $\mu\text{M}$  NHS-Silane solution for 60 min followed by subsequent removal of unbound compounds with 2-propanol. In a next step, the sensor was buffered in HEPES buffer (50 mM HEPES; pH 7.4). Subsequently, 100  $\mu\text{g}$  of Protein A or G was added on the NHS-Silane functionalized sensor surface for 1 h. Unbound proteins were removed by rinsing the sensor with HEPES buffer. Before binding different antibodies, the sensor surface was saturated with a casein blocking solution for 15 min to disable reactive sides. Finally, the antibody was captured by the Protein A or G<sup>8</sup>-modified surface by exposure to a 66 nM solution of antibody for 30 min. Unbound antibody particles were rinsed off for at least 30 min with HEPES buffer. According to the antibody subtype, monoclonal antibody A8978, and Tau-5 were applied to Protein A functionalized sensor surfaces, whereas the monoclonal antibody HJ5.1 was attached to a protein G functionalized sensor surface. For each preparative step, infrared-difference spectra were recorded. A detailed description can also be found in former publications.<sup>1,3</sup>

**Measurement of Synthetic  $\text{A}\beta$  and Recombinant Tau.** Synthetic  $\text{A}\beta$ (1–42) fibrils were prepared as described in Nabers et al.<sup>1</sup> Recombinant Tau was expressed at the Department of Biophysics (Bochum, Germany). Briefly, the gene coding for full-length Tau was transformed in BL21 DE3 cells. For plasmid selection, the cells were incubated on LB-agar plates containing 100  $\mu\text{g}/\text{mL}$  Kanamycin and 0.2% glucose at 37 °C overnight. A preculture (LB-medium, 100  $\mu\text{g}/\text{mL}$  Kanamycin, 0.2% glucose) was inoculated and incubated at 37 °C and 140 rpm overnight. For main culture, 4 L of LB was inoculated with the preculture and shaken in 1 L flasks. At an  $\text{OD}_{595}$  of 0.6, protein expression was induced using 1 mM 1-thio-L,D-galactopyranoside for 3.5 h. The cell pellet was resuspended in MES-KOH (50 mM MES, 500 mM NaCl, 1 mM  $\text{MgCl}_2$ , 5 mM DTT, pH 6.9) and boiled for 20 min at 100 °C. The homogenate was then centrifuged at 100 000g and 4 °C for 45 min. Finally, the supernatant was concentrated with a 30 kDa centrifugal filter.

20  $\mu\text{g}$   $\text{A}\beta$  fibrils or 100  $\mu\text{g}$  Tau were added to the antibody functionalized sensor surface in a circulating flow for 45 min. Unbound proteins were rinsed for 30 min with HEPES. For the measurements of synthetic  $\text{A}\beta$  peptides, the antibody A8978 (Sigma-Aldrich, Germany), whereas Tau-5 (ThermoFisher) was used as capture antibody for recombinant Tau.

**Measurement of CSF Samples.** Before any measurement, CSF samples were preincubated with 500  $\mu\text{g}$  Pierce Protein G Magnetic Beads, 500  $\mu\text{g}$  Pierce Protein A Magnetic Beads, and 500  $\mu\text{g}$  Pierce Protein A/G Magnetic Beads for 3 h at 7 °C in order to avoid binding of human IgGs from the sample to surface immobilized Protein A or G. For the immuno-infrared analysis, 100  $\mu\text{L}$  aliquots of CSF samples were circulated over the surface for 45 min in order to extract the  $\text{A}\beta$  peptide or Tau protein fraction from the body fluid. Remaining proteins of the CSF samples were rinsed for 30 min with HEPES buffer. Thus, only the  $\text{A}\beta$  or Tau secondary structure distribution in human CSF samples was detected. For the detection of  $\text{A}\beta$  from body fluids, monoclonal antibody HJ5.1 (Holtzman, Washington, USA) was used instead of A8978 because of the higher affinity to various  $\text{A}\beta$  conformational isoforms.

**Regeneration of the Sensor Surface.** For repeated measurements, the extracted  $\text{A}\beta$  or Tau fraction, as well as the antibody layer, were eluted from the sensor surface with 100 mM glycine (pH 2) for 10 min. The equilibration with HEPES buffer was finished after 10 min. Afterward, the protein A or G functionalized sensor surface was refreshed and could be used for a further antibody-binding process inclusive  $\text{A}\beta$  or Tau extraction from liquid solutions as described above.

**Fluorescence Analysis.** Before fluorescence analysis, the sensor surface was covalently functionalized with Protein A and rinsed with HEPES buffer as described above. Afterward, 5  $\mu\text{g}$  FITC-labeled monoclonal antibody 9F1 (Nanotools, Antikörpertechnik GmbH, Teningen, Germany) was incubated for 30 min and unbound antibodies were rinsed off with HEPES buffer. Fluorescence measurements were performed using the setup and protocols as previously published in Nabers et al.<sup>1</sup>

In summary, fluorescence signals were obtained through the quartz glass window (40 × 10 mm) of the ATR-flowthrough cell using a 100× magnification and 2 s exposure time. The FITC-labeled

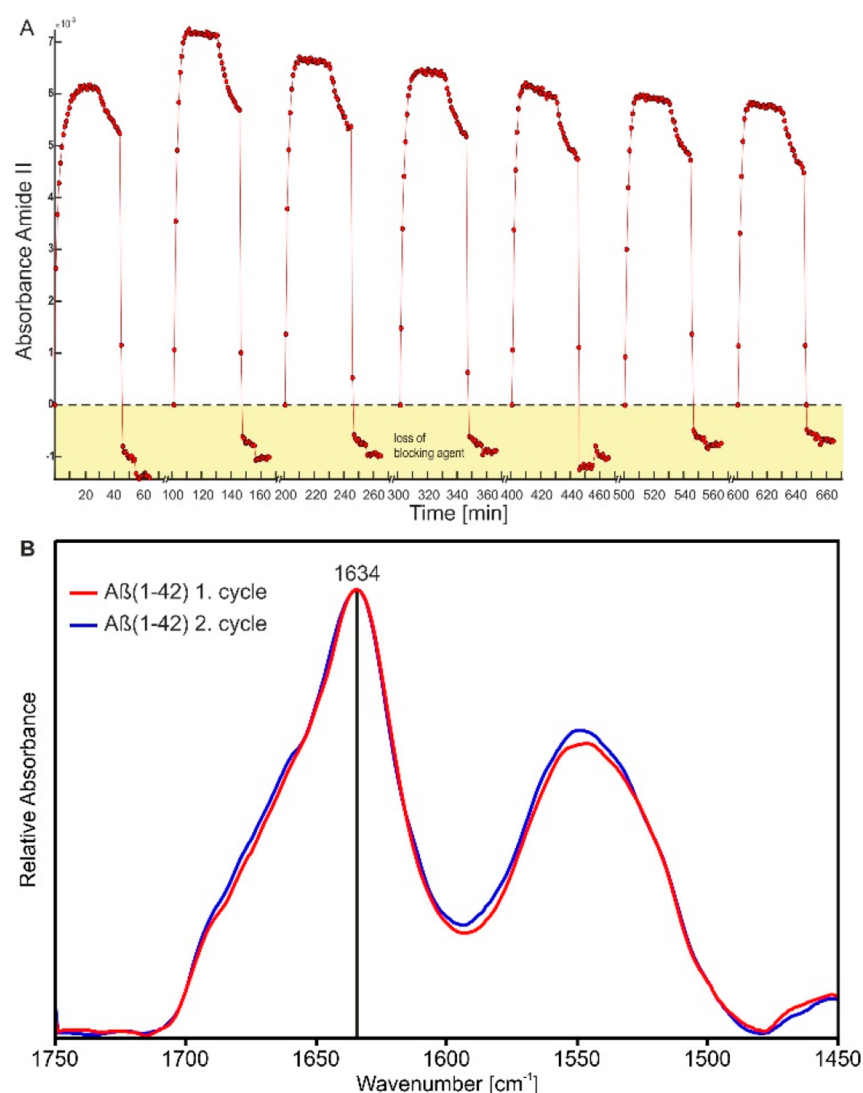


**Figure 2.** Repeated immobilization of antibody and reproducible binding of antigen. (A) Repetitive binding of antibody A8978 on the reversible immuno-infrared sensor surface. After binding of antibody at Protein A (30 min) and subsequent rinsing with HEPES buffer (15 min), the surface would be ready for antigen analysis. Here, we eluted the antibody via glycine pH 2 (10 min) followed by rinsing with buffer (10 min). This procedure was repeated 7 times. After each cycle, the surface was saturated with casein because of loss of blocking agent after antibody elution (see also Figure S5). (B) Synthetic A $\beta$ (1–42) was detected repeatedly with monoclonal antibody A8978 on Protein A. The resulting absorbance spectra of A $\beta$  were highly comparable with an identical amide I frequency at 1634 cm<sup>−1</sup>.

antibody was excited with 484 nm and emission was recorded at 518 nm. The contrast was enhanced by a factor of 3. As readout, we calculated the mean brightness value of all pixel of the green channel.

Subsequently, we again inserted the flow-cell in the spectrometer for further FTIR-measurements. Finally, the antibody bound to Protein A was eluted from the sensor surface with glycine pH 2 for 10 min and fluorescence intensity was recorded as described above.

## RESULTS AND DISCUSSION

The usage of Protein A and Protein G as noncovalent antibody capturing agents provides a reversible sensor surface for the repeated immobilization of different IgG antibodies in the immuno-infrared-assay. First, a self-assembled monolayer of NHS-silanes was generated with subsequent covalent immobilization of immunoglobulin binding proteins such as Protein A or Protein G (Figure 1, step zero; Figures S1, S2). The corresponding infrared spectra of Protein A and G, especially the amide I and II bands, are presented in Figure S3 and Figure S4, respectively. In the next step, unreacted esters or free

bindings sites on the sensor surface were blocked with casein (Figure 1, step one).<sup>1</sup> Subsequently, a specific antibody was added to the system (Figure 1, step two). The noncovalent immobilization of monoclonal antibody A8978 for A $\beta$  detection reached an absorbance plateau after 30 min. After rinsing for 15 min with HEPES buffer, sufficient amounts of immobilized antibodies remained on the sensor surface (Figure 2A). Now the sensor is ready for biomarker detection (Figure 1, step three). In general, antibody immobilization by Protein A or G was performed for 1 h with subsequent 30 min rinsing with HEPES to reveal an antibody absorbance plateau after washing (Figure S5). Only for the better illustration of repeated antibody immobilization cycles in Figure 2A, we reduced incubation and rinsing time.

The sensor surface can be reused after antibody elution by washing the surface with glycine (pH 2) for 10 min (Figure 1, step 4, Figure 2A). The following washing step with HEPES buffer revealed that the antibody layer was completely removed



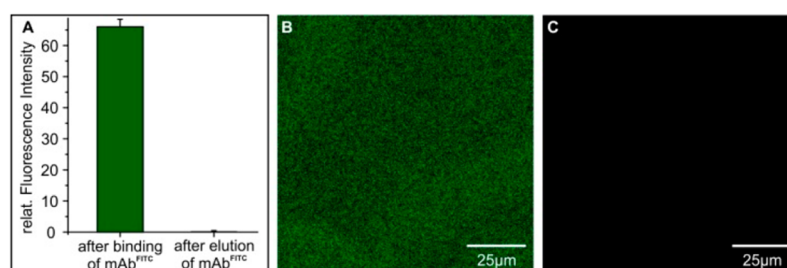


**Figure 3.** Validation of antibody immobilization and elution on the reversible immuno-infrared sensor by the fluorescence intensity of a FITC-labeled antibody 9F1 ( $\text{mAb}^{\text{FITC}}$ ). (A,B) Green fluorescence was recorded after  $\text{mAb}^{\text{FITC}}$  attachment on Protein A and subsequent rinsing with buffer (B). (A,C) After  $\text{mAb}^{\text{FITC}}$  elution with glycine pH 2 and buffer rinsing, no fluorescence intensity was observed (C) confirming the reversible character of the sensor surface.

(Figure 2A). The negative absorbance is caused by a loss of blocking agent as can be assigned by its spectral signature (Figure S6). Therefore, after elution, each cycle started with another saturation of free reactive sites on the sensor surface by casein. A full set of both raw data and processed data indicating the sensor functionalization is given in Figure S7. The reusability was investigated for seven cycles over 2 days. The amount of immobilized antibody decreased from a maximum of 7.2 mOD on cycle 2 to 6.1 mOD on cycle 7 (Figure 2A). However, even 35 cycles performed over 7 days were possible (Figure S8). The binding properties among the cycles do not change significantly as shown by the highly reproducible absorption spectra obtained after the extraction of synthetic fibrillar  $\text{A}\beta(1-42)$  by the monoclonal antibody A8978 (Figure 2B). Further evidence is the similarity of the Protein A spectrum before and after glycine treatment (Figure S9), and the similarity of the antibody spectra among the seven binding cycles (Figure S10). Thus, the sensor surface can be easily regenerated and used for repeated analyses in at least seven cycles without significant loss in performance. There is no need to dismantle the sensor from the spectrometer, followed by polishing, renewed surface activation, and surface functionalization. This saves measurement time, reduces user input, and makes system automation much easier.

For further validation of the elution of antibodies from the Protein A or G terminated surface, fluorescence analyses were performed: FITC-labeled monoclonal antibody 9F1 ( $\text{mAb}^{\text{FITC}}$ ) was attached to a Protein A terminated sensor surface in an identical manner as described above but directly under a fluorescence microscope. Fluorescence intensity was recorded during the binding and rinsing process, and after elution of the FITC-labeled antibody fraction. After the fluorescence intensity was stabilized in the washing step, the antibody was eluted using 100 mM glycine pH 2 for 10 min.

As shown in Figure 3, the relative green fluorescence intensity was 65.0 after immobilization of  $\text{mAb}^{\text{FITC}}$ . In contrast, after elution of the antibody fraction, the relative green fluorescence intensity was 0.0. These results confirmed the spectral results of the elution process highlighted in Figure 2A.

Most antibody immobilizations are done by unspecific adsorption or by covalent coupling of amine residues of the antibody to surface bound NHS-groups.<sup>2,13</sup> This leads to a random orientation of the antibody, and only a fraction will be able to bind the antigen. Especially surface binding via the N-termini of the antibody is disadvantageous, because they are close to the antigen binding site. In contrast, the immunoglobulin binding proteins used in our approach bind the antibody at the Fc region, leaving the Fab region

unperturbed. This leads to a 3–4-fold increase of antigen binding per immobilized antibody as shown in Figure S11. Note that the antibody spectra were very similar in both cases, suggesting a native antibody surface (Figure S12).

In a next step, we wanted to validate the reproducibility of the reversible surface for the analysis of the  $\text{A}\beta$  secondary structure distribution in CSF. Therefore, pooled CSF samples of AD patients and health control (HC) subjects were measured separately (Figure 4). The recorded  $\text{A}\beta$  IR-difference

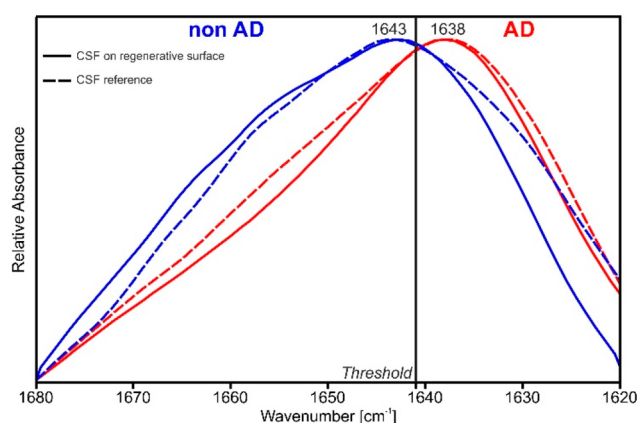


**Figure 4.** Reproducibility of the reversible sensor surface with  $\text{A}\beta$  from CSF in comparison with former results on a nonreversible surface as a control.  $\text{A}\beta$  from CSF as measured with antibody HJ5.1 on Protein G (solid lines) revealed results highly comparable to the literature (dashed lines).<sup>2</sup> For AD cases (in both cases maximum below the discriminative threshold) and HC subjects (both above the discriminative threshold), maxima were identical, indicating that the reversible immuno-infrared sensor can be used for AD diagnostics.

spectrum represents an integrated signal over all conformational  $\text{A}\beta$  isoforms present in the respective body fluid. This secondary structure distribution of all  $\text{A}\beta$  isoforms can be used in an immuno-infrared assay for the diagnosis of Alzheimer's disease (Figure 1, step 3).<sup>2</sup> In a former study, AD patients demonstrated a higher content of  $\beta$ -sheet enriched isoforms in the total  $\text{A}\beta$  fraction, resulting in a lower amide I maximum position as compared to disease control subjects. Thus, AD was detected by a simple threshold classifier with maxima below  $1642\text{ cm}^{-1}$  indicative for AD. Indeed, in the case of an AD sample the maximum of the amide I band of  $\text{A}\beta$  was  $1638\text{ cm}^{-1}$ , below the threshold. On the other hand, in the case of an HC CSF sample the corresponding maximum was  $1643\text{ cm}^{-1}$ , above the threshold. We compared these results with data of the same patient samples obtained with the former non-

reversible immuno-infrared assay. As shown in Figure 4, the amide I bands of A $\beta$  were highly comparable between both assays, and most importantly, the maxima of the amide I bands are identical, leading to the same diagnoses. Identical maxima were also obtained in measurements with synthetic A $\beta$  (Figure S13).

We could demonstrate that the reversible surface allows the extraction of A $\beta$  from CSF and thus the diagnosis of AD using a simple threshold classifier. The obtained results were in high agreement with former results received with the covalently linked antibody surface.<sup>1,3</sup> To further validate the regenerative sensor, we performed multiple A $\beta$  extractions from pooled CSF. It was possible to extract A $\beta$  from pooled CSF in successive cycles and between independent experiments with no loss in performance (Figures S14, S15). The average maximum of the detected amide I band of extracted A $\beta$  was  $1637.4\text{ cm}^{-1} \pm 0.6$  over 5 measurements (Figure S16). Thus, the regenerative sensor demonstrated lowest intermeasurement variabilities and can be used for screening in clinical studies.

Note that, as described in the Methods section (in SI), the complete removal of any IgG fractions within a sample is necessary for the reversible sensor, because IgG's could bind to free binding sites of the immobilized immunoglobulin binding proteins (Figure S17). Consequently, the recorded amide I band after A $\beta$  extraction would have strong spectral contributions from human IgG antibodies. This would lead to an absorbance downshift due to IgG's high content of  $\beta$ -sheet structures, interfering with diagnostics.

AD pathology is characterized by abnormal misfolding or altered concentration of different biomarkers, e.g., A $\beta$ , Tau, Neurofilament light chain (NFL), neurogranin, or YKL-40.<sup>14–16</sup> Levels of these biomarkers were determined in CSF and used as gold standard for AD neurochemical diagnostics. Appropriately, a reversible sensor could subsequently detect multiple biomarkers. Since the Tau protein is also known to undergo a structural change from monomeric to aggregated  $\beta$ -sheet enriched species, we used the reversible immuno-infrared sensor to detect both A $\beta$  and Tau, respectively. In a first step, monoclonal antibody Tau-5 was attached to the surface linked Protein A layer.

Therewith, recombinant Tau was extracted from a liquid solution in a monomeric state. After elution of Tau-5/Tau protein complexes from the surface, monoclonal antibody A8978 was attached to the Protein A layer to extract fibrillar A $\beta$  from an aqueous solution. We used monomeric Tau and fibrillar A $\beta$  as the two extreme protein conformations involved in AD pathology. Both conformations showed highly significant differences in the amide I region (Figure 5) which clearly demonstrated that the reversible immuno-infrared sensor can be used to successively detect different AD biomarkers and determine their secondary structure for diagnostic purposes.

## CONCLUSION

By employing immunoglobulin binding proteins such as Protein A and G as antibody capturing agents in an immuno-infrared assay, the workflow is convenient, saves cost, material, and time, and significantly increases the throughput of the method. Thus, this assay can be used as a biomarker screening tool, e.g., in clinical studies for early AD detection as demonstrated before.<sup>3</sup>

In contrast to assays where the capture antibodies are covalently linked to the sensor surface, the reversible setup has

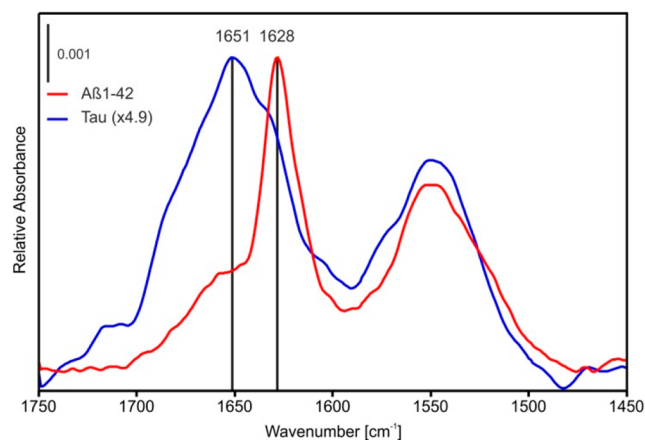


**Figure 5.** Detection of different AD biomarkers using the reversible immuno-infrared sensor. In a first step, antibody Tau-5 was immobilized on the Protein A coated sensor surface in order to capture recombinant Tau from aqueous solution. After elution of the antibody–antigen complexes, antibody A8978 was immobilized on the same sensor surface to capture fibrillar A $\beta$ (1–42) from aqueous solution. Between both steps, the sensor surface was saturated with casein for surface inertization (Figure 1).

a factor of 6 increased throughput with a highly comparable performance. The signal/noise is significantly improved due to the more specific immobilization of the antibody via the Fc region. Additionally, the reversible assay is completely automated and can be applied 24 h 7 days a week.

## ASSOCIATED CONTENT

### Supporting Information

The Supporting Information is available free of charge on the ACS Publications website at DOI: 10.1021/acssensors.9b00631.

Material and Methods; Binding kinetics; IR spectra; Spectral comparison of antibody elution and casein (PDF)

## AUTHOR INFORMATION

### Corresponding Author

\*E-mail: carsten.koetting@rub.de.

### ORCID

Brian Budde: 0000-0003-4244-5342

Jonas Schartner: 0000-0002-0797-3433

Lars Tönges: 0000-0001-6621-144X

Carsten Kötting: 0000-0002-3599-9657

### Author Contributions

The manuscript was written through contributions of all authors. All authors have given approval to the final version of the manuscript.

### Notes

The authors declare no competing financial interest.

## ACKNOWLEDGMENTS

This research was supported by the Protein Research Unit Ruhr within Europe (PURE), Ministry of Innovation, Science and Research of North-Rhine Westphalia, Germany. We acknowledge David Holtzman and employees for providing monoclonal antibody HJ5.1.

## ■ ABBREVIATIONS

AD, Alzheimer's Disease; HC, health control; A $\beta$ , Amyloid- $\beta$ ; ATR, attenuated total reflection; CSF, cerebrospinal fluid; IgG, Immunoglobulin; mOD, milli optical density; HEPES, 4-(2-hydroxyethyl)-1-piperazineethanesulfonic acid; FITC, Fluorescein isothiocyanate; mAb, monoclonal antibody; NHS-silane, N-hydroxy succinimidyl-ester triethoxysilane; NFL, Neurofilament light chain

## ■ REFERENCES

- (1) Nabers, A.; Ollesch, J.; Schartner, J.; Kötting, C.; Genius, J.; Haußmann, U.; Klafki, H.; Wiltfang, J.; Gerwert, K. An infrared sensor analysing label-free the secondary structure of the A $\beta$  peptide in presence of complex fluids. *J. Biophotonics* **2016**, *9*, 224–234.
- (2) Nabers, A.; Ollesch, J.; Schartner, J.; Kötting, C.; Genius, J.; Hafermann, H.; Klafki, H.; Gerwert, K.; Wiltfang, J. Amyloid- $\beta$ -Secondary Structure Distribution in Cerebrospinal Fluid and Blood Measured by an Immuno-Infrared-Sensor: A Biomarker Candidate for Alzheimer's Disease. *Anal. Chem.* **2016**, *88*, 2755–2762.
- (3) Nabers, A.; Perna, L.; Lange, J.; Mons, U.; Schartner, J.; Güldenaupt, J.; Saum, K.; Janelidze, S.; Holleczek, B.; Rujescu, D.; et al. Amyloid blood biomarker detects Alzheimer's disease. *EMBO Mol. Med.* **2018**, *10*, No. e8763.
- (4) Nabers, A.; Hafermann, H.; Wiltfang, J.; Gerwert, K. A $\beta$  and tau structure-based biomarkers for a blood- and CSF-based two-step recruitment strategy to identify patients with dementia due to Alzheimer's disease. *Alzheimer's Dement. Diagnosis, Assess. Dis. Monit.* **2019**, *11*, 257–263.
- (5) Rigler, P.; Ulrich, W. P.; Hoffmann, P.; Mayer, M.; Vogel, H. Reversible immobilization of peptides: Surface modification and in situ detection by attenuated total reflection FTIR spectroscopy. *ChemPhysChem* **2003**, *4*, 268–275.
- (6) Rusmini, F.; Zhong, Z.; Feijen, J. Protein immobilization strategies for protein biochips. *Biomacromolecules* **2007**, *8*, 1775–1789.
- (7) Bonroy, K.; Frederix, F.; Reekmans, G.; Dewolf, E.; De Palma, R.; Borghs, G.; Declerck, P.; Goddeeris, B. Comparison of random and oriented immobilisation of antibody fragments on mixed self-assembled monolayers. *J. Immunol. Methods* **2006**, *312*, 167–181.
- (8) Kihira, Y.; Aiba, S. Artificial immunoglobulin G-binding protein mimetic to staphylococcal protein A. Its production and application to affinity purification of immunoglobulin G. *J. Chromatogr. A* **1992**, *597*, 277–283.
- (9) Cohen, S.; Sweeney, H. M. Modulation of protein A formation in *Staphylococcus aureus* by genetic determinants for methicillin resistance. *J. Bacteriol.* **1979**, *140*, 1028–1035.
- (10) Akerström, B.; Brodin, T.; Reis, K.; Björck, L. Protein G: a powerful tool for binding and detection of monoclonal and polyclonal antibodies. *J. Immunol.* **1985**, *135*, 2589–92.
- (11) Akerstrom, B.; Bjorck, L. a Physicochemical Study of Protein-G, a Molecule With Unique Immunoglobulin-G-Binding Properties. *J. Biol. Chem.* **1986**, *261*, 240–247.
- (12) Kim, D.; Herr, A. E. Protein immobilization techniques for microfluidic assays. *Biomicrofluidics* **2013**, *7*, 041501.
- (13) Schartner, J.; Güldenaupt, J.; Mei, B.; Rögner, M.; Muhler, M.; Gerwert, K.; Kötting, C. Universal method for protein immobilization on chemically functionalized germanium investigated by ATR-FTIR difference spectroscopy. *J. Am. Chem. Soc.* **2013**, *135*, 4079–4087.
- (14) Hampel, H.; Toschi, N.; Baldacci, F.; Zetterberg, H.; Blennow, K.; Kilimann, I.; Teipel, S. J.; Cavedo, E.; Melo dos Santos, A.; Epelbaum, S.; et al. Alzheimer's disease biomarker-guided diagnostic workflow using the added value of six combined cerebrospinal fluid candidates: A $\beta$ 1–42, total-tau, phosphorylated-tau, NFL, neurogranin, and YKL-40. *Alzheimer's Dementia* **2018**, *14*, 492–501.
- (15) Olsson, B.; Lautner, R.; Andreasson, U.; Öhrfelt, A.; Portelius, E.; Bjerke, M.; Hölttä, M.; Rosén, C.; Olsson, C.; Strobel, G.; et al. CSF and blood biomarkers for the diagnosis of Alzheimer's disease: a systematic review and meta-analysis. *Lancet Neurol.* **2016**, *15*, 673–684.
- (16) Sutphen, C. L.; Jasielec, M. S.; Shah, A. R.; Macy, E. M.; Xiong, C.; Vlassenko, A. G.; Benzinger, T. L. S.; Stoops, E. E. J.; Vanderstichele, H. M. J.; Brix, B.; et al. Longitudinal cerebrospinal fluid biomarker changes in preclinical Alzheimer disease during middle age. *JAMA Neurol.* **2015**, *72*, 1029–1042.

## **Supporting Information**

### **Reversible Immuno-Infrared-Sensor for the Detection of Alzheimer's Disease Related Biomarkers**

Brian Budde<sup>†,‡</sup>, Jonas Schartner<sup>†</sup>, Lars Tönges<sup>§,‡</sup>, Carsten Kötting<sup>\*,‡</sup>, Andreas Nabers<sup>†,‡</sup>, Klaus Gerwert<sup>†,‡</sup>

<sup>†</sup>Department of Biophysics, Ruhr-Universität Bochum, Universitätsstr. 150, 44801 Bochum, Germany

<sup>§</sup>Dept. of Neurology, Ruhr-University Bochum, St. Josef-Hospital, Gudrunstr. 56, 44791 Bochum, Germany

<sup>‡</sup>Center for Protein Diagnostics (ProDi), Gesundheitscampus 4, 44801 Bochum, Germany

\*Corresponding author: Carsten Kötting, Tel.: +49 234 32 18069, E-Mail: [carsten.koetting@rub.de](mailto:carsten.koetting@rub.de)

#### **Table of Contents**

**S1: Binding kinetics of covalently immobilized protein A**

**S2: Binding kinetics of covalently immobilized protein G**

**S3: IR spectrum of covalently immobilized protein A**

**S4: IR spectrum and binding kinetics of covalently immobilized protein G**

**S5: Long-term binding kinetics of antibody A8978**

**S6: Spectral comparison of antibody elution and casein**

**S7: Compilation of infrared spectra recorded during the sensor functionalization, elution, and recovery of an antibody functionalized reversible immuno-infrared-sensor surface**

**S8: Final state of the Amide II absorbance in different cycles of binding and elution of immobilized antibody A8978 immobilized on Protein A**

**S9: Influence of elution buffer on protein A**

**S10: Comparison of antibody spectra during repeated immobilization**

**S11: Comparison of the binding capacities for the current sensor and the regenerative sensor**

**S12: Comparison of antibody spectra immobilized on NHS-silane and protein A**

**S13: Immobilized A $\beta$  on current system and regenerative surface**

**S14: Comparison of the detection of A $\beta$  from pooled CSF in the first cycle of antibody binding and elution and the last cycle within a measurement**

**S15: Comparison of the detection of A $\beta$  from pooled CSF in different cycles of antibody binding and elution**

**S16: Mean spectrum and standard deviation of pooled AD CSF samples**

**S17: Spectral quality control of IgG depletion from CSF**

## Material and Methods

### Data acquisition and preprocessing

Immuno-infrared-analyses were performed using a Vertex 70V FTIR-spectrometer (Bruker Optics GmbH, Ettlingen, Germany) with an integrated ATR unit “GS11000 – 25 Reflection Variable Incidence Angle ATR” (Specac Ltd., Slough, England) as described previously.[1–3] The set-up can be used in a completely automatized and parallelized manner as described in detail by Nabers, Perna et al.[3] However, the recorded infrared difference spectra were corrected from spectral traces of atmospheric water vapour by scaled subtraction of a reference spectrum. Furthermore, high frequency noise was removed by a Fourier low pass filter.[1] Kinetic analyses were performed after baseline correction of all spectra.[1]

### CSF procedures

A permission of the local ethics committees has been obtained prior to the initiation of the study. Written consent was provided by all patients or care givers. The study conforms to the Code of Ethics of the World Medical Association (Declaration of Helsinki). CSF samples were analyzed from AD patients (Duisburg-Essen cohort, ethical board of the University of Duisburg-Essen, # 12 5160 BO) or from patients with a neurodegenerative disease but not AD (Bochum cohort; ethical board of Ruhr University Bochum, # 17-6119). According to a previously published protocol, all patients underwent a lumbar puncture, where 10 mL of CSF were collected in polypropylene tubes and treated in a standard procedure. Routine testing included WBC and RBC count, protein and lactate levels. CSF was immediately centrifuged (2000 g; 20 min; 4°C) within 30 min of collection and frozen at -80°C until further analysis. Samples with a RBC count > 100/ IL in the routine testing sample were excluded.[4]

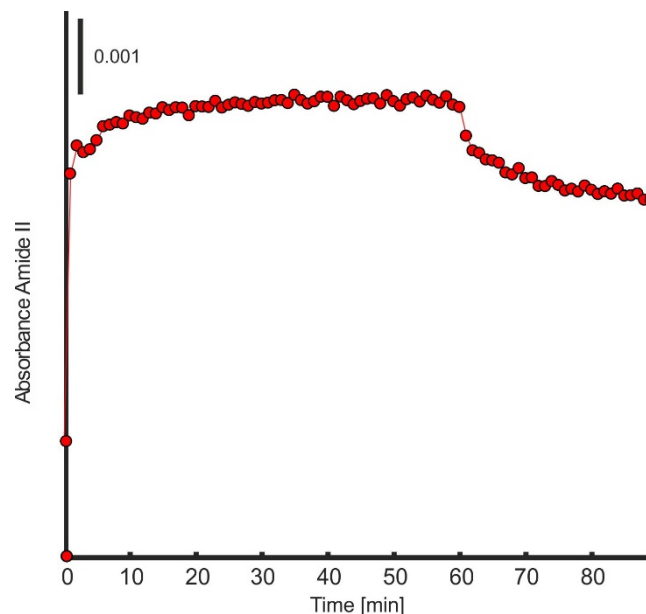


Figure S1: Binding kinetic of 100 µg Protein A immobilized on the NHS-silane modified immuno-infrared-sensor surface.



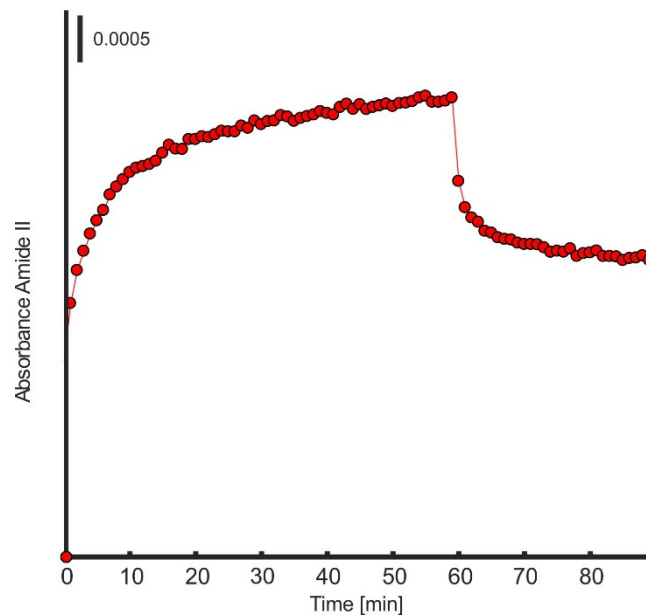


Figure S2: Binding kinetic of 100  $\mu\text{g}$  Protein G immobilized on the NHS-silane modified modified immuno-infrared-sensor surface.

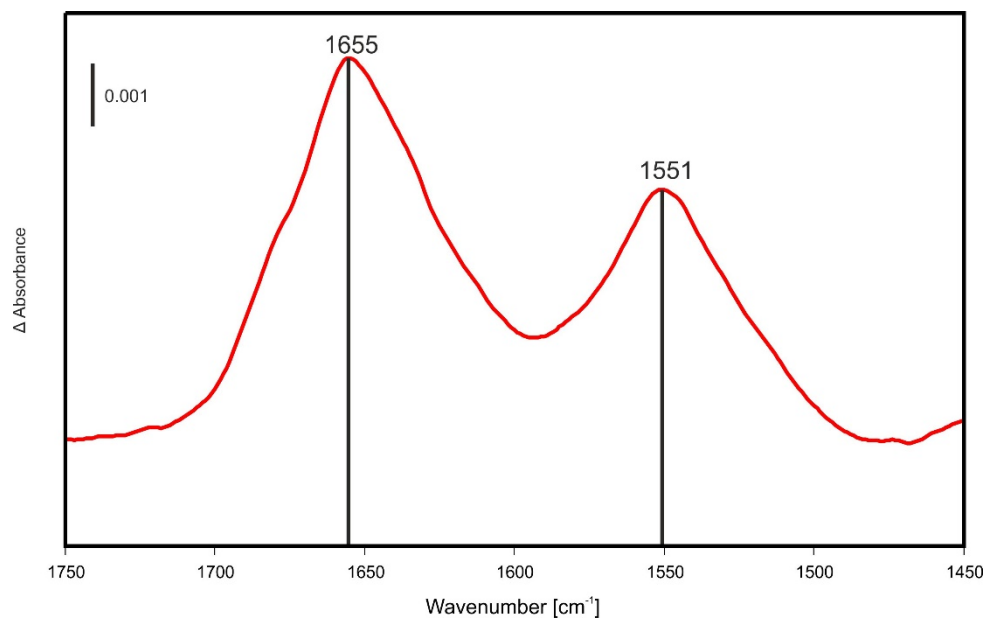


Figure S3: Difference absorbance spectrum of covalently immobilized Protein A on the NHS-silane terminated immuno-infrared-sensor surface. The spectrum was recorded after 60 min immobilization and subsequent rinsing with buffer for 30 min (last dot of Figure S1).

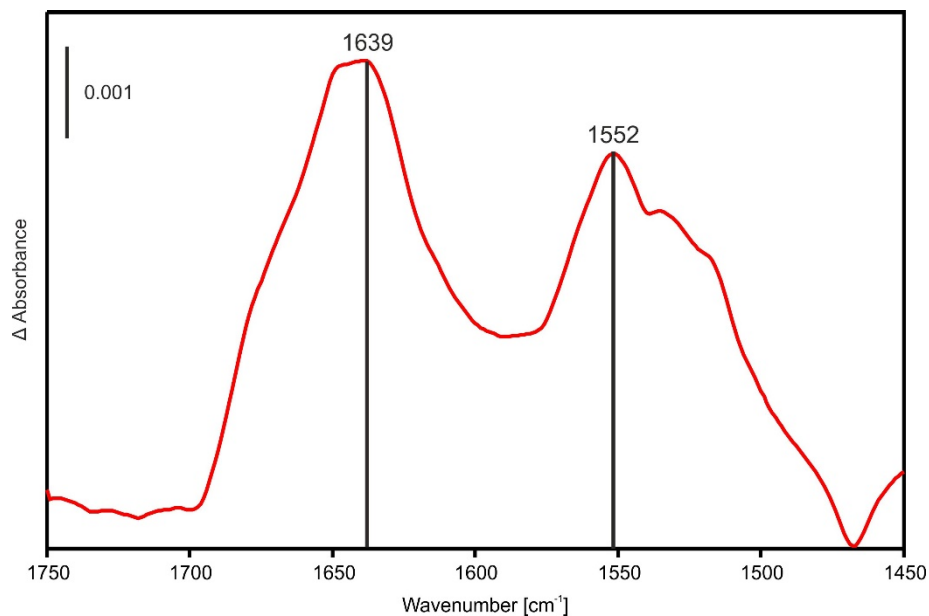


Figure S4: Difference absorbance spectrum of covalently immobilized Protein G on the NHS-silane terminated immuno-infrared-sensor surface. The spectrum was recorded after 60 min immobilization and subsequent rinsing with buffer for 30 min (last dot of Figure S2).

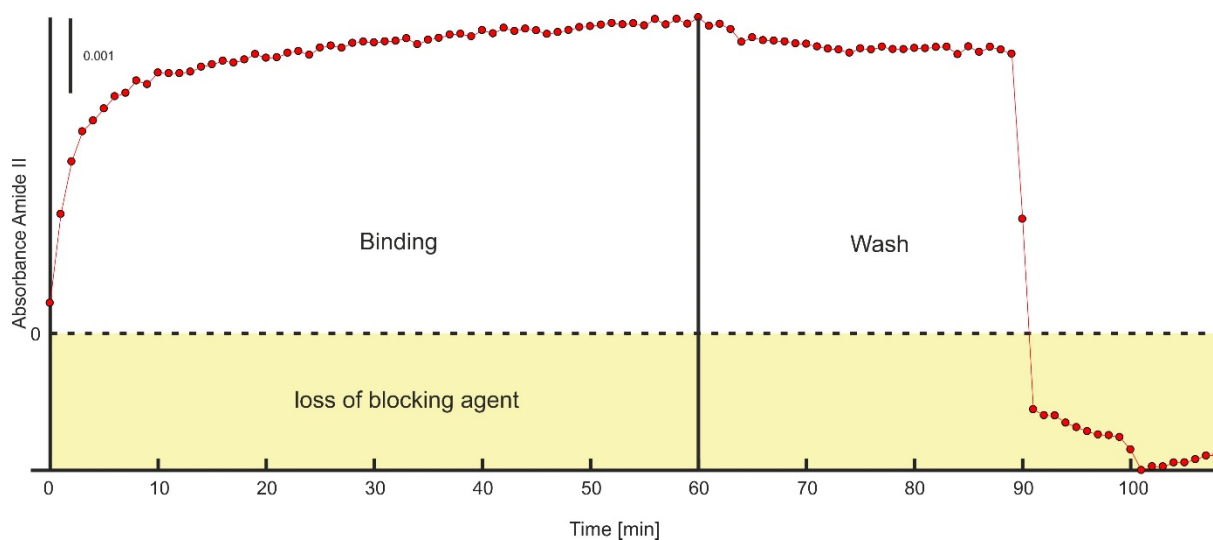


Figure S5: Binding kinetic of antibody A8978 immobilized on Protein A. The antibody was incubated for 60 min followed by 30 min excessive rinsing with HEPES buffer. Finally, the antibody was eluted with glycine pH 2 for 10 min with subsequent buffer rinsing.

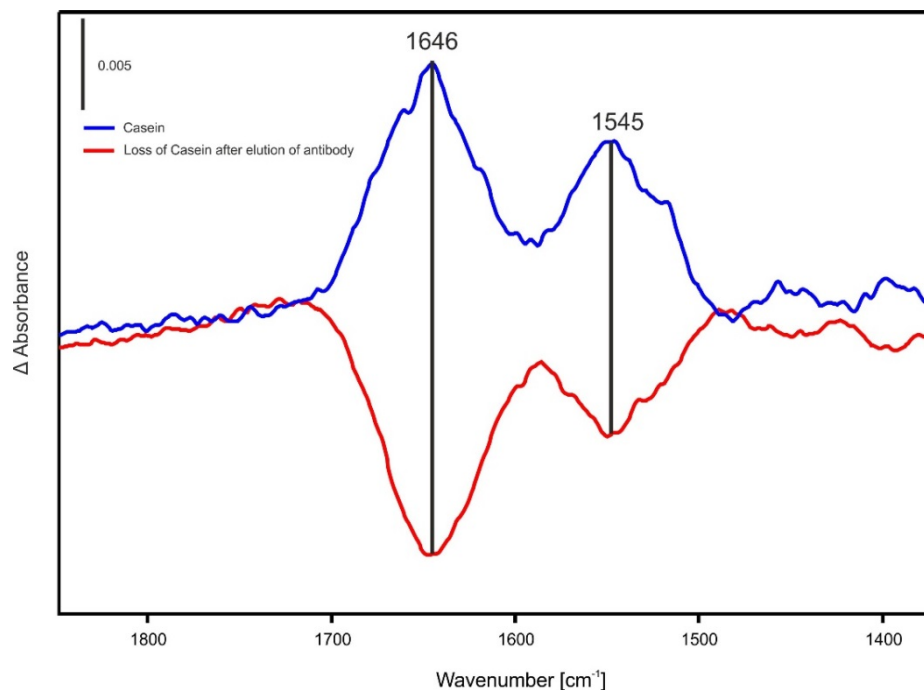


Figure S6: Comparison of the difference spectrum of casein (blue; Casein spectrum was recorded during the blocking procedure, see also Figure 1 step 1) and the difference spectrum obtained after elution of the antibody-antigen complex (red). After eluting the antibody A8978 from the regenerative sensor surface (linked to Protein A) with glycine pH 2 a negative difference signal was obtained (red, see also Figure 2). Since the elution buffer has no influence on Protein A or G (see Figure S8) and their corresponding spectra the negative difference signal after elution is caused by the loss of Casein. About 75% of the blocking agent detaches from the germanium surface after the elution process.

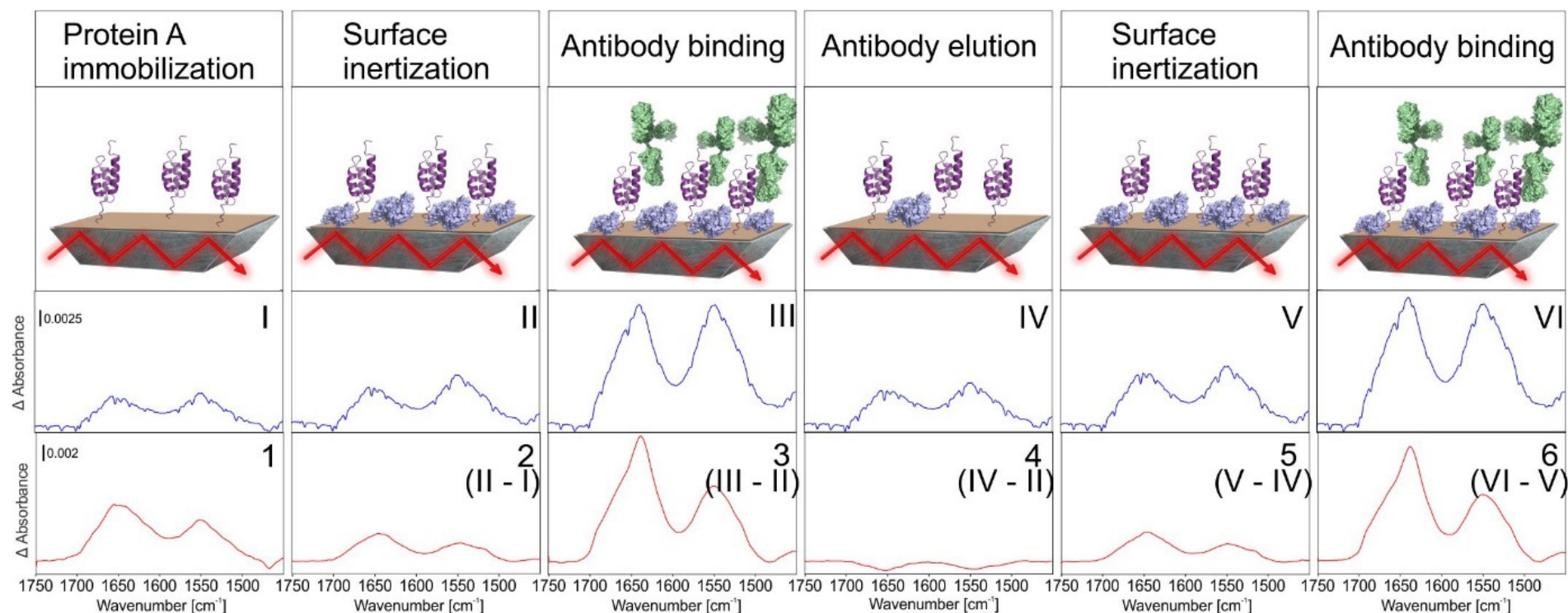


Figure S7: Compilation of infrared spectra recorded during the sensor functionalization, elution, and recovery of an antibody functionalized reversible immuno-infrared-sensor surface. Raw data (in blue) of protein A (I), casein blocking reagent (II,V), monoclonal antibody (III,VI), and surface elution (IV) were calculated based on the same background spectrum recorded before surface modification with protein A (I). Processed difference spectra (corrected for water vapor and baseline drift, see methods) are shown in red. For calculation of these difference spectra (1-6) a respective reference spectrum was recorded immediately before each new procedural step. Thus, each step of the functionalization was resolved at molecular level providing characteristic spectra of the added analyte (protein A, casein, antibody).



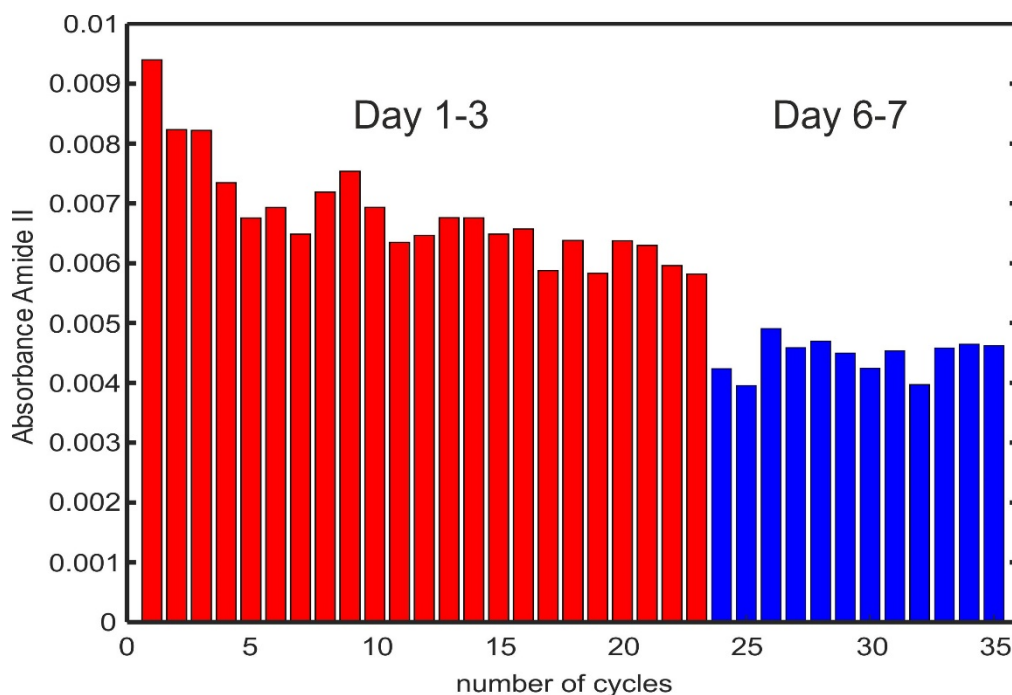


Figure S8: Final state of the Amide II absorbance in different cycles of binding and elution of immobilized antibody A8978 immobilized on Protein A. The antibody A8978 was bound for 30 minutes on the protein A terminated and Casein blocked surface, followed by a 15 minute washing step with 50 mM HEPES buffer. The antibody was eluted using 100 mM glycine pH 2, followed by a 10 minute washing step with 50 mM HEPES buffer. The surface needs to be blocked with 0,1% Casein before the next cycles are performed to prevent any unspecific interactions between the antibody and the surface.

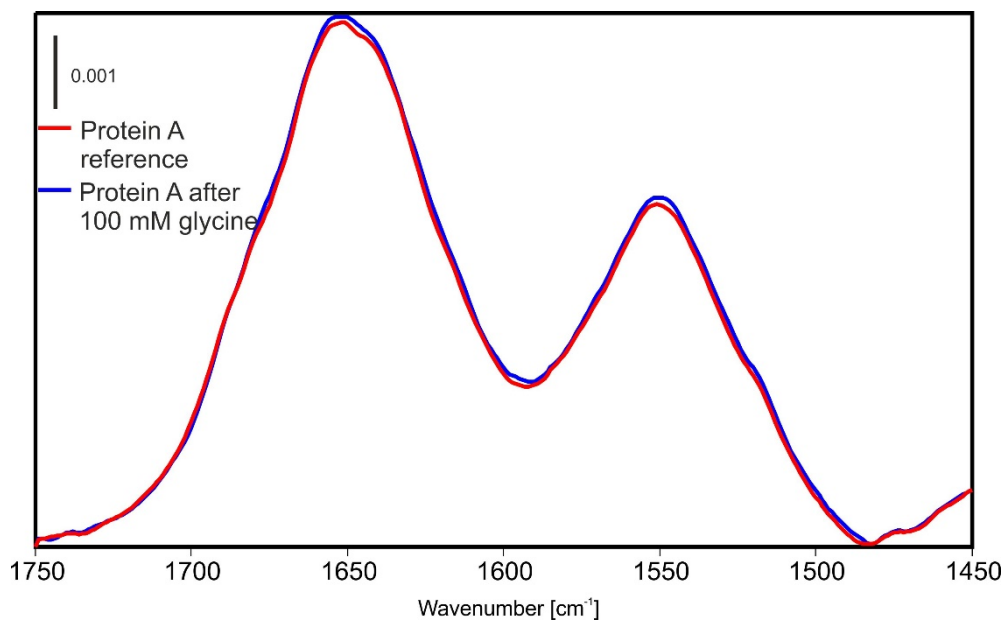


Figure S9: Comparison of immobilized Protein A before (red) and after (blue) treatment with 100 mM glycine pH 2. The elution buffer has no influence on the Protein A secondary structure.

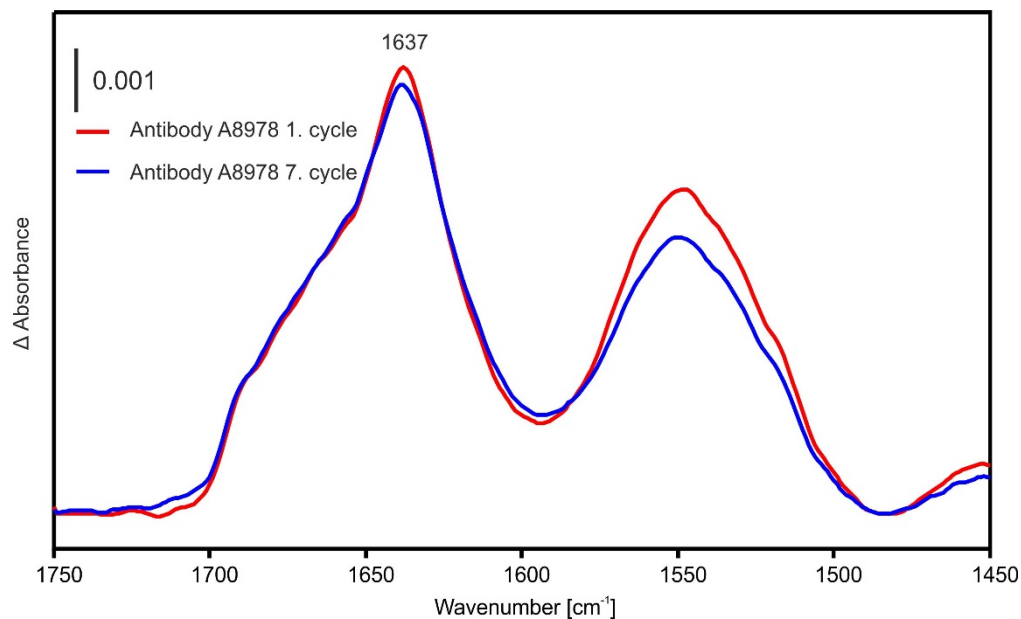


Figure S10: Comparison of the antibody difference spectra immobilized on protein A. The binding of the antibody was repeated 7 times. The spectrum of the first immobilization is shown in red, the spectrum of the seventh immobilization is shown in blue.

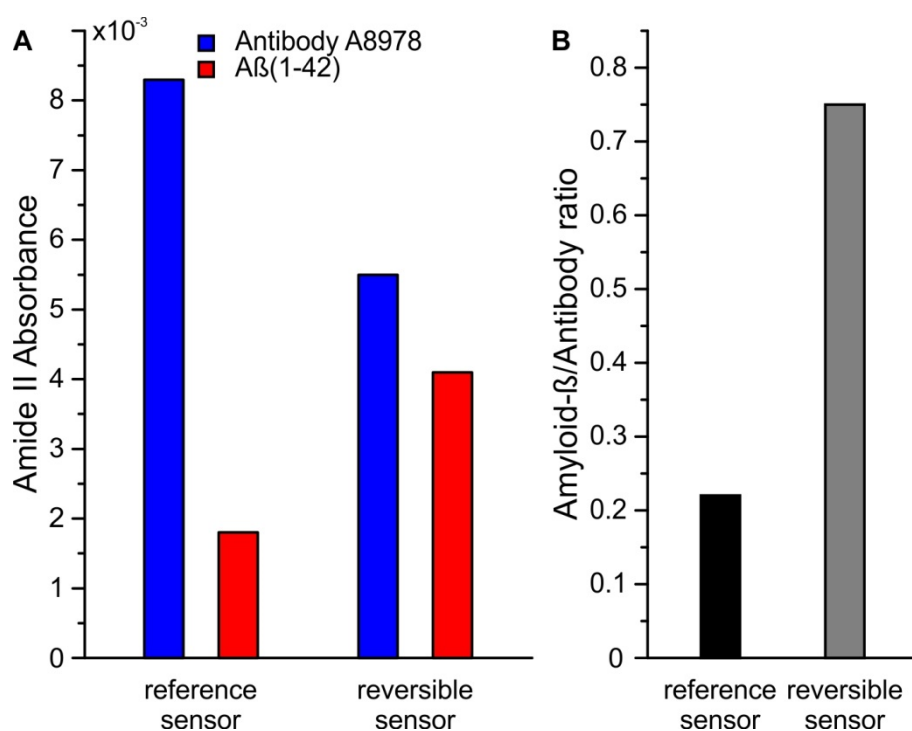


Figure S11: (A) Comparison of the immobilization of capture antibody A8978 (blue) and Aβ (red) for the reference sensor and the reversible sensor. (B) Aβ-antibody ratios for the reference sensor and the regenerative system. The regenerative systems shows a 3.5 fold higher binding capacity for the capture antibody.

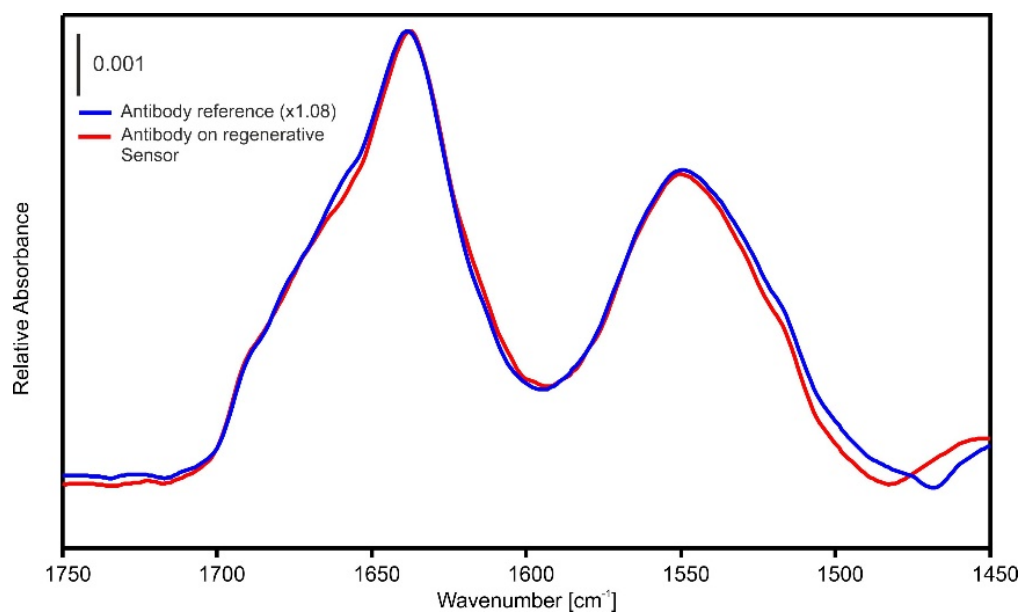


Figure S12: Difference absorbance spectra of antibody A8978 covalently attached on NHS-silanes as described previously[1–3] (antibody reference, blue) and reversibly immobilized on Protein A (red). Both immobilization methods provided identical antibody spectra, thus, the reversible sensor surface does not influence the antibody nature.

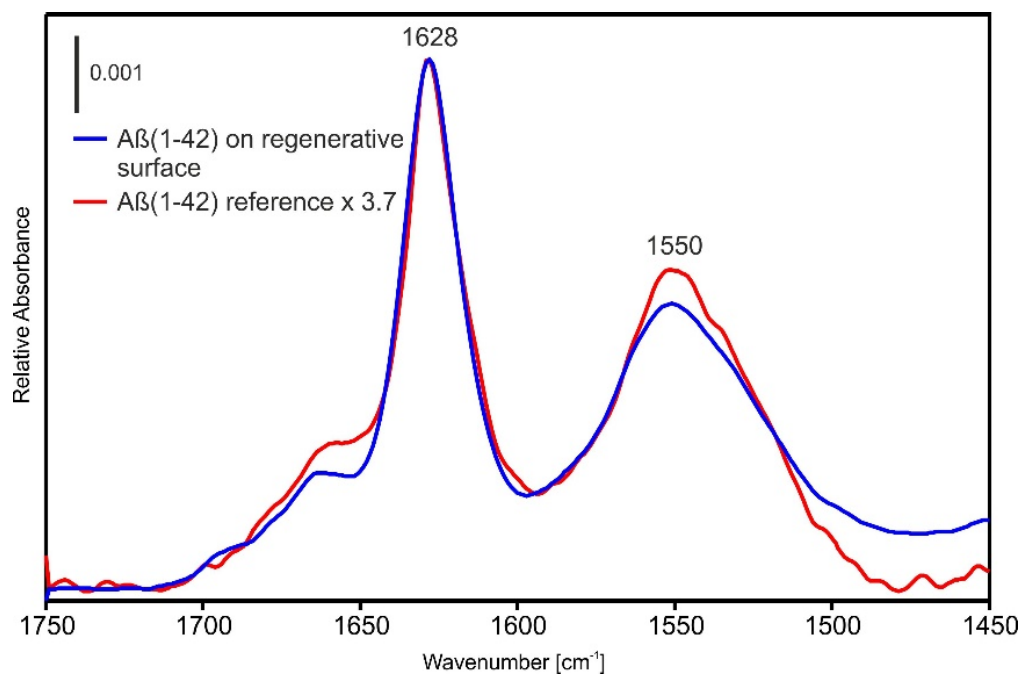


Figure S13: Comparison of A $\beta$ (1-42) fibrils captured on covalently attached antibodies as described previously[1] (red) or attached on the regenerative immuno-infrared-sensor surface (blue).

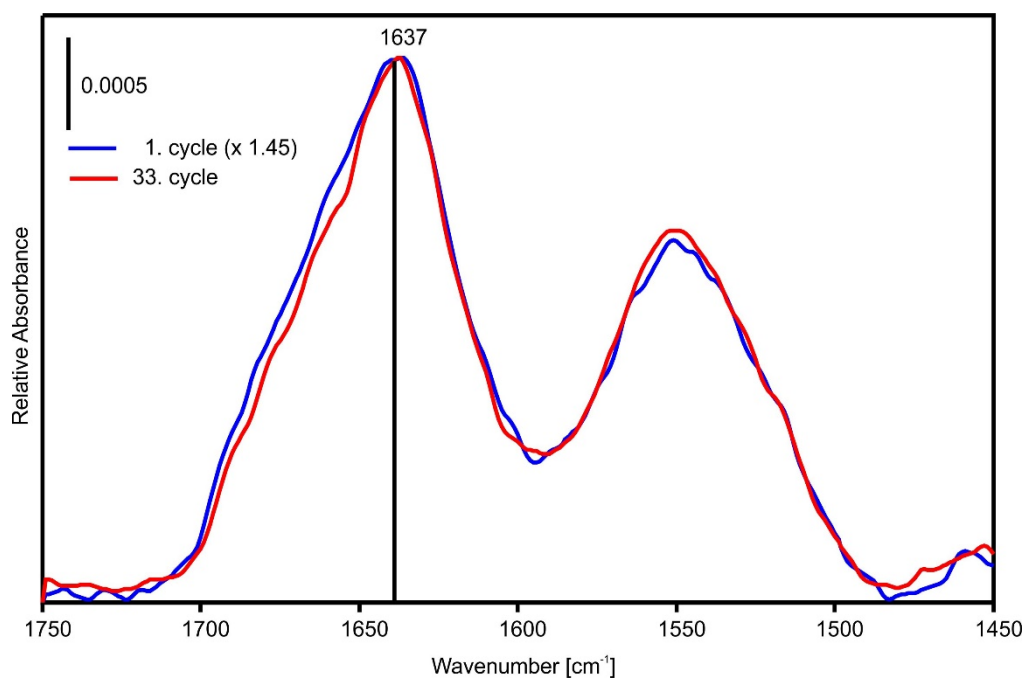


Figure S14: Detection of A $\beta$  from pooled CSF in different cycles of independent measurements. Thus, the regenerative sensor demonstrated highest reproducibility within one experiment comprising several cycles (see S14) and among different measurements (minimal inter-measurement variability).

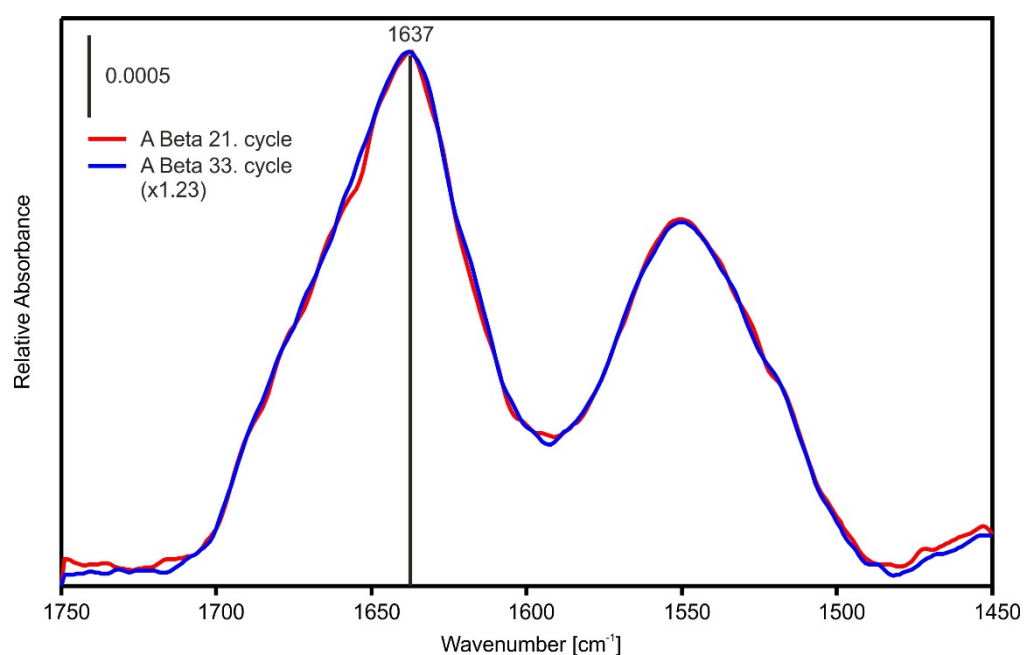


Figure S15: Comparison of the detection of A $\beta$  from pooled CSF in different cycles of antibody binding and elution. For these measurements the antibody A8978 was used.



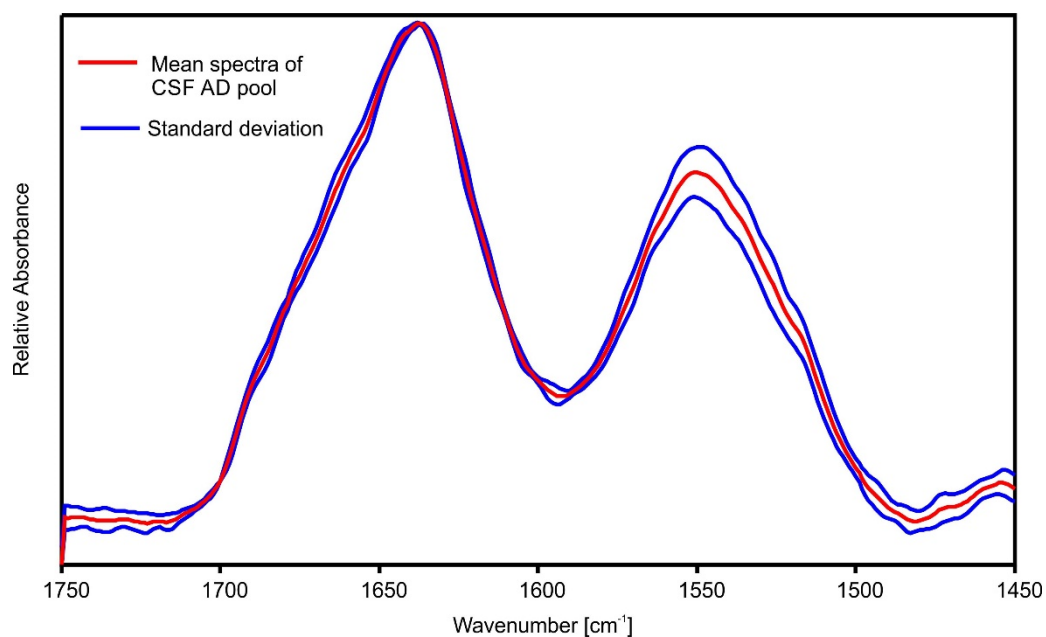


Figure S16: Mean spectrum (red) and standard deviation (blue) of normalized spectra of pooled AD CSF samples. In total, five A $\beta$  extractions were performed using the antibody A8978. The maximum of the mean spectrum is at 1637.4 cm<sup>-1</sup>. The standard deviation is +/- 0.6 cm<sup>-1</sup>.

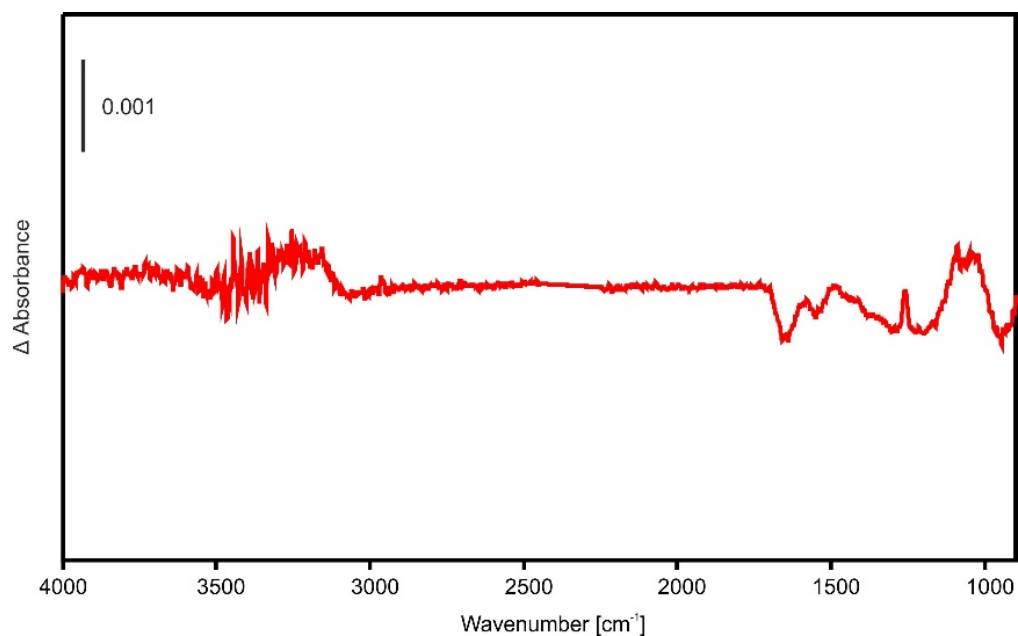


Figure S17: Spectral quality control of the success of complete IgG depletion from a CSF sample. Therefore, 100  $\mu$ l CSF were pre-processed as described above (Measurement of CSF samples) and 10  $\mu$ l therefrom were circulated over a Protein A terminated and with casein blocked sensor-surface to substantiate the efficiency of IgG depletion. As a result, no positive protein difference absorbance bands were detected in the amide region, thus, the IgG depletion was successful.

## References

1. Nabers, A.; Ollesch, J.; Schartner, J.; Kötting, C.; Genius, J.; Haußmann, U.; Klafki, H.; Wiltfang, J.; Gerwert, K. An infrared sensor analysing label-free the secondary structure of the Abeta peptide in presence of complex fluids. *J. Biophotonics* **2016**, *9*, 224–234.
2. Nabers, A.; Ollesch, J.; Schartner, J.; Kötting, C.; Genius, J.; Hafermann, H.; Klafki, H.; Gerwert, K.; Wiltfang, J. Amyloid- $\beta$ -Secondary Structure Distribution in Cerebrospinal Fluid and Blood Measured by an Immuno-Infrared-Sensor: A Biomarker Candidate for Alzheimer's Disease. *Anal. Chem.* **2016**, *88*, 2755–2762.
3. Nabers, A.; Perna, L.; Lange, J.; Mons, U.; Schartner, J.; Güldenhaupt, J.; Saum, K.; Janelidze, S.; Holleczek, B.; Rujescu, D.; et al. Amyloid blood biomarker detects Alzheimer's disease. *EMBO Mol. Med.* **2018**, *10*, e8763.
4. Maass, F.; Michalke, B.; Leha, A.; Boerger, M.; Zerr, I.; Koch, J.-C.; Tönges, L.; Bähr, M.; Lingor, P. Elemental fingerprint as a cerebrospinal fluid biomarker for the diagnosis of Parkinson's disease. *J. Neurochem.* **2018**, *145*, 342–351.